J. Indian Chem. Soc.,
Vol. 94, November 2017, pp. 1203-1212

Clean green synthesis of silver nanoparticles with shape/size control using aquatic weed *Pistia stratiotes* and their antioxidant, antibacterial and catalytic activity

S. U. Ganaie, R. Rajalakshmi, Tasneem Abbasi*[#] and S. A. Abbasi

Centre for Pollution Control and Environmental Engineering, Pondicherry University, Puducherry-605 014, India

E-mail : tasneem.abbasi@gmail.com

Manuscript received 20 June 2017, revised 19 July 2017, accepted 17 November 2017

Abstract : The paper presents studies towards development of simple, one-pot, yet rapid processes of generating silver nanoparticles of desired shapes/sizes utilizing the highly invasive aquatic weed, *Pistia stratiotes*. In an attempt to utilize the entire plant, the extracts of all its parts – aerial as well as submerged parts – were employed with the silver precursor, $AgNO_3$ solution, for the synthesis. The formation of AgNPs and their characteristics were studied using UV-Vis spectroscopy, electron microscopy, Fourier transform infrared spectroscopy, Energy dispersive spectroscopy and X-ray diffraction. It was seen that by varying Ag-extract stoi-chiometry, pH and temperature AgNPs of different shapes and sizes can be reproductively generated. The synthesized AgNPs displayed marked antimicrobial, catalytic and free radical scavenging ability.

Keywords : Silver nanoparticles, *Pistia stratiotes*, antioxidant, antibacterial and catalytic activity.

Introduction

The thrust of nanotechnology is built around nanoparticles which play highly specialized roles owing to their unique optoelectronic and physico-chemical properties in bio sensing, media recording, optics, catalysis, environmental remediation, imaging, drug delivery, diagnostics, tissue engineering and gene delivery[1,2]. Silver nanoparticles (AgNPs), in particular, are distinguished by their biocompatibility and unique structural, electronic, magnetic, optical and catalytic properties. Hence synthesis of different forms of AgNPs in an economical and eco-friendly manner forms an important thrust area of nanotechnology[3].

Although existing chemical and physical methods have successfully produced well-defined nanoparticles, these processes often require high temperatures/pressures, and/or high energy inputs, and involve hazardous chemicals either as reducing agents and/or as stabilizing agents for the nanoparticles (NPs) formation. The physical conditions required for NPs generation is highly intensive and expensive; and the use of toxic chemicals in the synthesis process releases hazardous byproduct that may affect the environment in addition to human health. Consequently, the bio inspired AgNP synthesis is gaining importance not only due to its low cost and high reproducibility, but also its eco-friendliness[4]. Recently there have been numerous reports on extra-cellular AgNPs synthesis using living organisms such as actinomycetes, bacteria, fungi, algae[5], and/or vascular plant extracts[6,7]. Of these the phyto-fabrication of NPs is beneficial over the other bio agents because it is rapid and convenient[8,9]. It is not constrained by the need for elaborate and fine maintenance that characterize microorganism-base NP synthesis method. These are

[#]Concurrently visiting Associate Professor, Department of Fire Protection Engineering, Worcester Polytechnic Institute, Worcester, MA 01609, USA.

also free from the risk of microbial contamination; and are appropriate for large scale NPs synthesis[10–13]. Several plant species have been explored for their potential to generate AgNPs but most of the studies have employed species encompassing fruits, vegetables, cereals, spices, medicinal and other foodstuff, which already have well-established uses and entail substantial costs of production[14–17].

Pistia (*P. stratiotes*) is a free-floating pleustonic-macrophyte belonging to the Araceae family. It is one among the world's worst weeds and is now widespread in the lakes and ponds of the warmer parts of the world. In India, it is distributed throughout the tropical and subtropical regions of the country. Similar in appearance to the form salvinia (*Salvinia molesta*)[18], it also has a high growth-rate and forms dense mats on the surface of the water. As a consequence, the water flow in irrigation and drainage canals is hampered, the water outlets in dams are blocked, and navigation in large river systems is hindered. There is a serious harm to water quality[19,20]. Pistia also provides a habitat favorable to breeding of mosquitoes. Pistia has been explored for use in biogas generation[21], ethanol production[22], wastewater treatment[23,24] as an animal feed, green leaf manure, and a source of medicines[25]. Attempts have also been made to use it as an ornamental plant biosorbent for heavy metal removal, and as a substrate for vermicomposting[26]. However, none of the potential uses have been economically viable at a scale large enough for Pistia to be used as a means to manage and reduce the spread of the weed[27,28]. Hence the present work was undertaken with the dual objective of finding a freely available plant for AgNPs which also indirectly providing an incentive for harvesting. Pistia, thereby exerting control over its proliferation and adverse impacts.

Experimental

All chemicals were analytical reagent grade unless otherwise specified. Deionized water, double distilled in all-glass stills, was used throughout.

Preparation of aqueous extracts of aerial part of the plant :

Aerial and submerged parts of the weed Pistia (*P. stratiotes*) were collected from ponds in or near the Pondicherry University campus, Puducherry. The plant parts were washed with water to knock off adhering fauna and muck. They were then disinfected by dipping in highly saline water. After rinsing off the salinity, the plants were blotted dry, and chopped to pieces of average length 4 ± 2 cm. Large pooled samples of these pieces were taken, weighed, and left to dry in the oven at 105 °C to constant weights[29]. Based on the 'dry weight' thus obtained, extracts for nanoparticle synthesis were made by boiling dry weight equivalents of the plant material at concentrations of 20 g/L for 5 min. The resulting slurry was filtered through a Whatman no. 42 filter paper and the filtrate was stored under refrigeration at 4 °C. Reconnoitery experiments indicated that the extracts retained their integrity for up to 6 days, as evidenced by the optical density at λ_{max} of nanoparticles generated by them. Hence in all the experiments the extracts were used within 6 days of preparation.

Ag^{1+} solution :

A 10^{-3} *M* stock solution of Ag^{1+} was prepared using $AgNO_3$ and was stored in dark.

Synthesis of silver nanoparticles :

The synthesis involved mixing extract-metal concentrations varying in ratios spanning 1 : 0.05 to 1 : 0.075 at ambient temperature and pressure to see their influence on the shapes and sizes of the AgNPs that were formed. A change seen in the appearance of the reactant mixture from almost colorless to brown gave a visual indication of the commencement of the AgNP formation. The progress of the synthesis was followed continuously by monitoring the UV-Visible spectrum of the reactant mixture. The color and its intensity seemed to depend on the plant part used and stoichiometric ratio in which the plant extract and the metal ion had been mixed[30].

Characterization of the synthesized AgNPs :

UV-Visible spectroscopy : The silver nanoparticle formation was monitored by recording the UV-Vis spectra in the range of 190–1100 nm for the reaction mixture filled in quartz cuvettes with 1 cm path length. Water was used as blank. ELICO (model SL164) double beam UV-Visible spectrophotometer was employed for the purpose[30].

Electron microscopic (SEM, HR-SEM, TEM) and EDAX studies of the synthesized AgNPs : SEM (scanning electron microscope) of Hitachi, S-3400N make, HR-SEM (high resolution scanning electron microscope) of FEI Quanta, FEG 200 make and TEM (transmission electron microscope) of JEOL, JEM-2100 make were used to determine the size, shape and morphology of the synthesized AgNPs. The AgNPs present in the mixture of the plant extract and the unreduced metal ion solution mixture were centrifuged at 12,000 rpm for 20 min using Remi C 24 centrifuge. The resulting pellets were washed thrice with water to remove the unreacted constituents and were re-dispersed in water. The samples for SEM studies were prepared by placing a drop of the AgNP suspension on a carbon-coated SEM grid. For HR-SEM studies the samples were prepared by placing dried pellets of AgNPs on a carbon coated aluminum stub. For TEM studies the AgNPs were pelletized by diluting and through sonication. The micrographs were recorded by depositing a drop of the well dispersed samples on carbon coated 300 mesh placed on copper TEM grids and excess liquid was wiped off with filter paper[31].

EDAX attached with the HR-SEM instrument provided information about the purity of the particles by determining their elemental composition. The EDX spectrum was recorded after documenting the electron micrographs in the spot profile mode by focusing on the densely occupied AgNP region[31].

X-Ray diffraction (XRD) studies : The powder XRD (X-Ray Diffraction) spectrum of the AgNPs was recorded to investigate the crystallinity of the nanoparticles. An aliquot of the pelletized AgNPs was drop-casted to thin film on a glass slide and the spectral recording was executed by scanning in the 2θ region, from 0° to 80°, at 0.02° per minute, and with the time constant of 2 s. The crystalline pattern of the nanoparticles was recorded using CuKα1 radiation with a wavelength (λ) of 1.5406 Å at a tube voltage of 40 kV and a tube current of 30 mA[32].

Fourier transform infrared spectroscopic (FTIR) studies : FT-IR spectroscopic studies were used to identify the functional groups involved in the stabilization of the AgNPs. For performing the FT-IR studies, the samples were dried completely and ground with potassium bromide[32]. The spectrum was recorded at diffuse reflectance mode with 4 cm^{-1} resolution in the mid-IR region between the wavenumbers 4000 and 400 cm^{-1}.

Results and discussion

The core process :

On adding the plant extract to the Ag^{1+} solution in select proportions, AgNP formation commenced, with the gradual appearance of the characteristic shades of brown AgNP colors. These colors are known to appear due to the localized surface plasmon resonance (SPR) exhibited by the combined vibration of free conduction electrons of AgNPs when it is induced by light[33]. Sharp or broad single absorption bands occurred depending on the plant part used for preparing the extract and its concentration with respect to Ag^{1+}. With aerial extract a single sharp peak was obtained after 216 h of incubation while extracts of the submerged plant part gave a broad absorption peak after 168 h (Fig. 1). The sharp peak is evidently exhibited by small sized spherical nanoparticles. This was confirmed from the SEM and TEM studies, which showed that the size of particles synthesized using the aerial extract were indeed small and mostly spherical in shape. On the other hand the presence of broad absorption bands as in submerged extracts indicated that

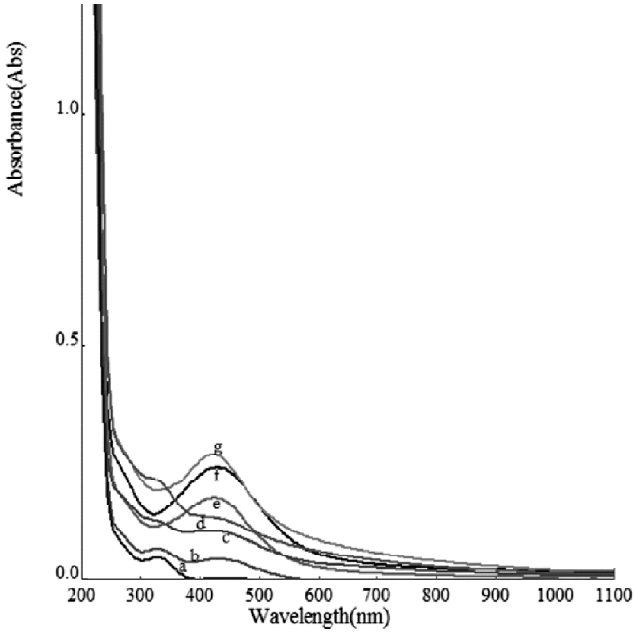

Fig. 1. UV-Vis spectra recorded for silver nanoparticles synthesized using identical Ag^{1+} concentration (25 mg/L) and extract of aerial part of *P. stratiotes* concentration : (a) 25 mg/L, (b) 50 mg/L, (c) 75 mg/L, (d) 100 mg/L, (e) 125 mg/L, (f) 150 mg/L, (g) 175 mg/L.

the synthesized particles possessed an intrinsic anisotropy. This was also confirmed by the SEM and TEM studies.

The results obtained from the UV-Visible spectral studies further revealed that the optical density of the nanoparticles was found to increase gradually with an increase in the time and concentration of Ag^{1+} till 1 : 0.07 extract-metal ratios and started decreasing thereafter.

When the concentration of Ag^{1+} ions relative to the extract concentration was changed from 0.25 fold to 15 fold, it caused an increase in the absorbance at λ_{max}, signifying that the rate of formation of AgNPs had increased (Fig. 2). The change in the shape of the spectra from broad and asymmetric to narrow and symmetric also indicated an increasing shift towards monodispersion of the nanoparticles.

As the temperature of the reactants was increased to 70 °C, there was a decrease in the rate of AgNP formation, as was reflected in a decrease in the optical density of all Ag^{1+}-extract combinations irrespective of the Ag^{1+}-extract proportions used for the synthesis of AgNPs. The effect of pH was studied over the 2–12 unit range.

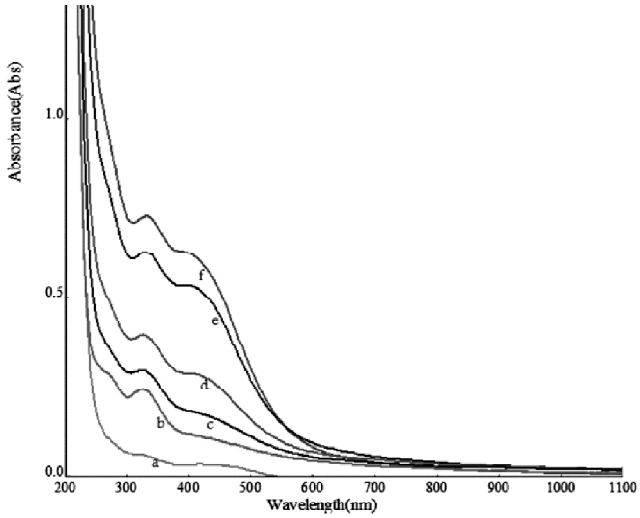

Fig. 2. UV-Vis spectra recorded for silver nanoparticles synthesized using identical extract of aerial part of *P. stratiotes* concentration (400 mg/L) and Ag^{1+} concentration : (a) 8 mg/L, (b) 25 mg/L, (c) 50 mg/L, (d) 75 mg/L, (e) 100 mg/L, (f) 125 mg/L.

There was no AgNP formation at pH 2–4. Subsequently, as the pH was increased, the AgNP formation commenced after 24 h at approximately pH 6. A further rise in the pH from 7 to 10 led to formation of nanoparticles within minutes after the addition of NaOH. This increase in the rate of nanoparticle formation was accomplished by a gradual change in the shape of the absorption peak from broad and asymmetric to increasingly narrow and symmetric. This signifies that a rise in the pH leads to the synthesis of larger quantities of nanoparticles with a concomitant decrease in their size. A further increase in pH to 10 caused the destabilization of the nanoparticles and appearance of turbidity.

FTIR studies revealed that carbonyl, hydroxyl and amine groups of proteins in the extracts of both the aerial and submerged parts of Pistia have been mainly responsible for the reduction and stabilization of AgNPs.

Crystallinity :

The powder XRD analysis was used to determine the crystalline structure of the synthesized AgNPs. The diffractograms (Fig. 4) have intense peaks at the 2θ position, matching with (111), (200), (220) and (113) Bragg's planes and indicating a face centered cubic structure of the nanoparticles. The broadening of Bragg's peaks indicates the formation of nanoparticles. The mean size of silver nanoparticles was calculated using Scherrer equation,

$$D = \frac{0.9\lambda}{\beta \cos \theta}$$

where D is the mean grain size, λ is the X-ray wavelength for CuKα (λ = 1.5406 Å), β is FWHM of diffraction peak, and θ is the diffraction angle. The average particle sizes of the AgNPs calculated using Debye-Scherrer equation were found to be 32 nm ((111) Bragg reflection[34] which coincides with the SEM results.

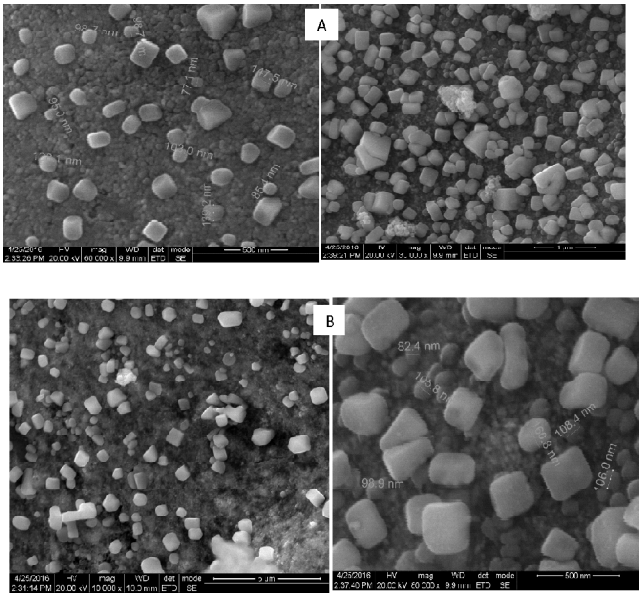

Fig. 3. SEM micrographs of the AgNPs generated (A) using extract of part of *P. stratiotes* at extract-Ag^{1+} ratio 1 : 0.05; and (B) using extract of submerged part of *P. stratiotes* at the same extract-Ag^{1+} ratio.

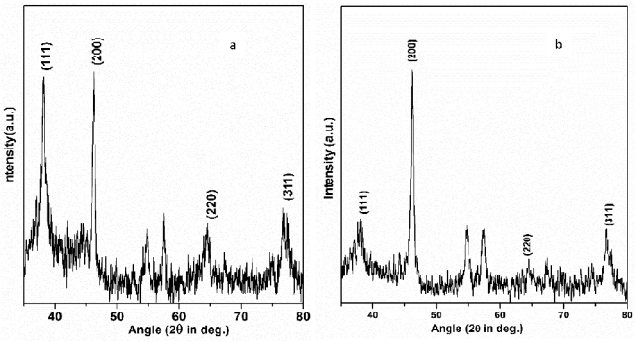

Fig. 4. X-Ray diffraction spectra of AgNPs : (a) synthesized using extract of aerial part of *P. stratiotes* at extract-Ag^{1+} ratio 1 : 0.05 and (b) using extract of submerged part of *P. stratiotes* at the same extract-Ag^{1+} ratios as respectively.

Shapes and sizes of the AgNPs :

The elemental composition of the AgNPs was assayed using EDAX. A strong clear peak seen in spot-profile mode of the EDAX spectrum (Fig. 5) at approximately 3 keV confirms the presence of Ag. Weak signals from carbon atoms are also seen that may be due to the biomolecules involved in the capping of the AgNPs. The TEM micrographs indicates that depending on the metal-extract stoichiometry either isotropic spherical AgNPs are formed or there is an anisotropy resulting in a mixture of spherical, triangular, tetrahedral, pentagonal, hexagonal and irregular shapes (Fig. 6). The TEM images also point to the microstructure and crystalline nature of the AgNPs. The bright circular spots recorded in the SAED patterns corresponding to the Bragg's planes confirm the highly crystalline nature of all types of AgNPs.

HR-SEM micrographs (Fig. 3) of AgNPs revealed that nanoparticles with sizes ranging 10–60 nm are formed with extract of aerial parts of Pistia while particles of larger sizes, ranging 40–81 nm, are formed when the extracts of the weed's submerged parts are used (Fig. 7). The size distribution among the AgNPs formed with Pistia is shown in Fig. 3. Aerial extracts predominantly form AgNPs in the size range 11–20 nm (61%), followed by AgNPs in the size range 21–

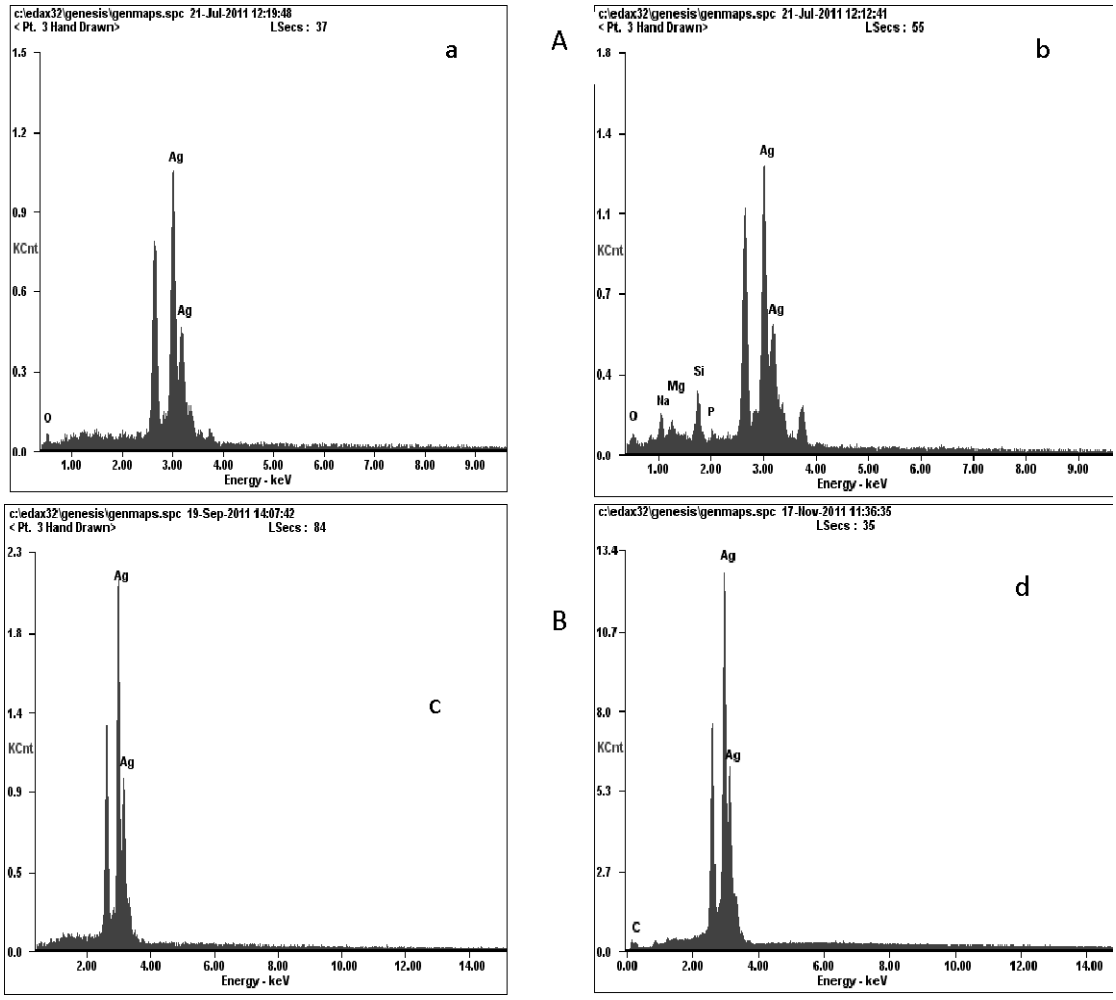

Fig. 5. EDAX spectrum of the AgNPs : (A) synthesized using extract of aerial part of *P. stratiotes* at extract-Ag^{1+} ratio (a) 1 : 0.05, (b) 1 : 0.075; (B) using extract of submerged part of *P. stratiotes* at the same extract-Ag^{1+} ratio (c) 1 : 0.05, (d) 1 : 0.075.

30 nm (14%). In contrast the submerged parts predominantly generate AgNPs in the 41–50 nm range (58%). Further analysis of size distribution indicated that 26% of the AgNPs formed within 11–20 nm range belonged to 17 or 18 nm size which 35% of the AgNPs of the 41–50 nm range had the size 56 or 57 nm. The submerged parts also lead to AgNPs of greater polydispersity (36%) than the aerial parts (22%). These findings can be useful in determining which part to be used to generate AgNPs of which predominant size range. The average size of NPs generated using submerged parts of Pistia (19.8 nm) was also slightly greater than the NPs synthesized using aerial parts (18.0 nm).

Free radical scavenging activity :

Free radicals are formed in animal body by exotic chemicals or endogenous metabolic processes. The free radicals are capable of oxidizing life-sustaining biomolecules such as nucleic acids, proteins, lipids and DNA, thereby denaturizing the biomolecules. This can lead to degenerative diseases like neurological disorders, cancer, emphysema, cirrhosis, atherosclerosis and arthritis. The free radicals can be destroyed by antioxidants. Due to this, there is strong thrust towards finding safe, effective and cheap antioxidants.

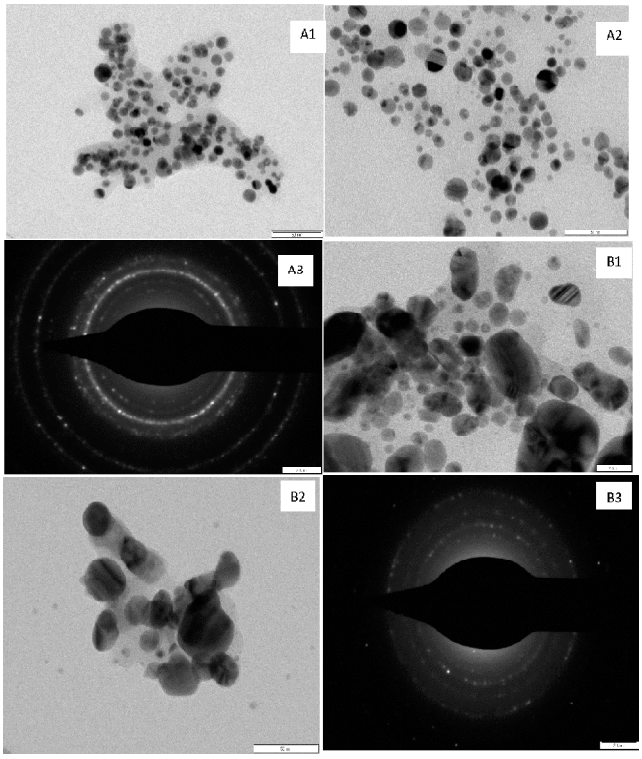

Fig. 6. TEM micrographs of the AgNPs (A 1-3) generated using extract of aerial part of *P. stratiotes* at extract-Ag^{1+} ratio 1 : 0.05 and (B 1-3) generated using extract of submerged part of *P. stratiotes* at the same extract-Ag^{1+} ratio.

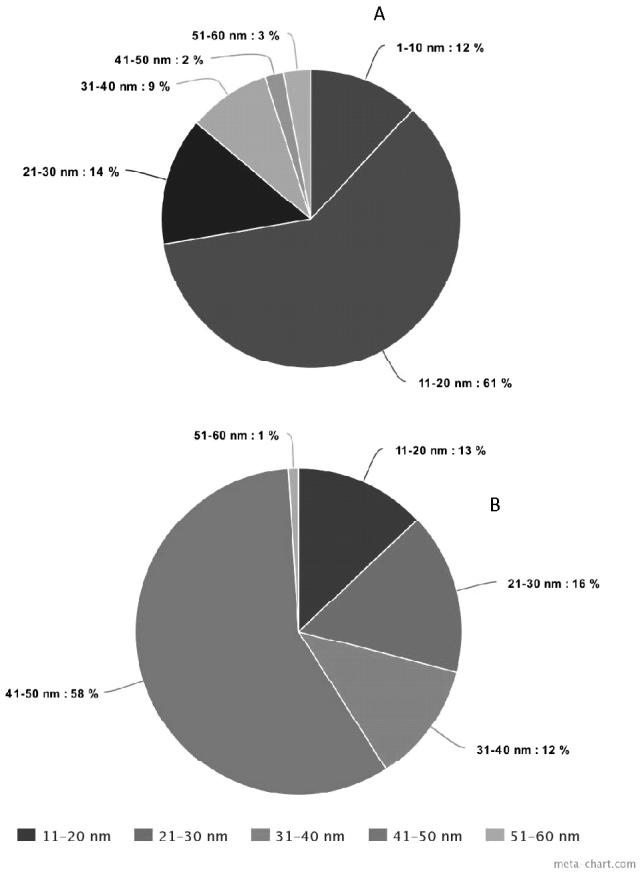

Fig. 7. Size distribution of AgNPs synthesized (A) using extract of aerial part and (B) extract of submerged part of *P. stratiotes*.

Keeping this in view antioxidant activity of aerial and submerged parts of *P. stratiotes* and AgNPs was assayed by DPPH assay[35].

The results are summarized in Fig. 10. As may be seen, the aerial extracts exhibit the highest antioxidant activity followed by submerged extracts (Fig. 8). The aerial extract-AgNP combinations had higher scavenging activity (98.39%) than the extract (81.9%) and this activity increased in a dose dependent manner. The possible reasons for the greater tendency of extract-AgNPs to reduce DPPH may be their high surface area to volume ratio and the presence of antioxidant biomoities on their surfaces[36].

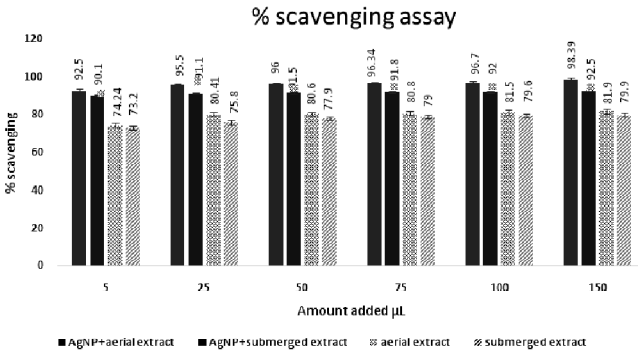

Fig. 8. Comparison of free radical scavenging activity with respect to different applied volumes of extract of aerial and submerged part of *P. stratiotes* and of AgNPs synthesized using the extracts.

Antimicrobial activity :

Pathogenic strains of *Escherichia coli* and *Staphylococcus aureus* were used to test the antibacterial activity of Ag NPs by the standard Kirby-Bauer disc diffusion assay[27]. The bacterial cultures were grown in Luria-Bertani (LB) broth for 18 h on agar plates which had been sterilized and allowed to solidify, 50 µL cultures of each organism were spread. Sterilized

Whatman no. 42 filter paper disc of 6 mm were then placed on the agar plates and freshly prepared Ag NP suspensions of volumes 25 µL, 50 µL, 100 µL and 150 µL were loaded onto each disc. A disc loaded with 150 µL of plant extract served as a control. The agar plates were then incubated at 37 °C for 24 h, the results were deemed positive when distinct zones of inhibition observed around the discs after the incubation period.

It may be seen (Fig. 10) that zones of inhibition are formed around discs loaded with Ag NPs in case of both the Gram (+) and Gram (–) bacteria while no such zone is seen around the control disc. The inhibition of Gram (–) bacteria appears to be stronger than that of the Gram (+) bacteria.

Catalytic activity :

4-Nitro phenol (4-NP) gets reduced to 4-aminophenol only if a catalyst is present along with a reducing agent (such as sodium borohydride). To see whether the synthesized AgNPs catalyze this reaction, the reaction was studied in the presence and absence of AgNPs. To a mixture containing 0.8 mL of sodium borohydride (0.1 mM) and 1 mL of 4-NP (0.1 mM), 200 µL of AgNPs were added in the reaction tube. The volume of the mixture was made up to 3 mL with distilled water and the progress of the reaction was monitored spectrometrically. For the uncatalyzed reaction 200 µL of AgNPs were replaced by an equal amount of water. A 4-NP solution to which neither sodium borohydride nor AgNPs were added, served as yet another control (Fig. 9)[38].

The aqueous solution of 4-NP exhibited a characteristic absorption peak at 317 nm (Fig. 9a). Upon addition of $NaBH_4$, a red shift of the peak from 317 to 400 nm was observed due to the formation of 4-nitrophenolate ion (Fig. 9b). This peak remained constant for a week and more reflecting the stability of the 4-nitrophenolate ion. But as soon as AgNPs were added to the reaction mixture, catalytic reduction started and the gradual formation of 4-AP caused the 400 nm peak to shift to 290 nm (Fig. 9c). It was thus established that the evidently AgNPs possess catalytic activity. They perhaps facilitated electron relay from the donor BH_4^- to the acceptor 4-NP; it helping

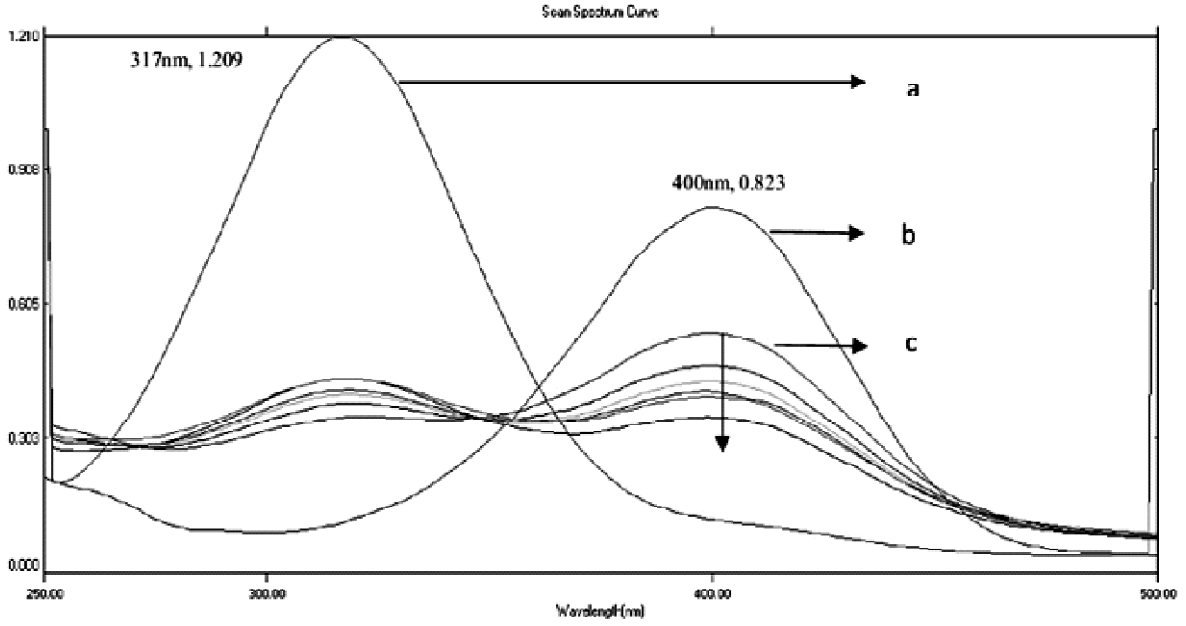

Fig. 9. UV/Vis spectra of 4-NP (a) before adding $NaBH_4$, (b) after adding $NaBH_4$ and (c) after adding AgNPs+$NaBH_4$.

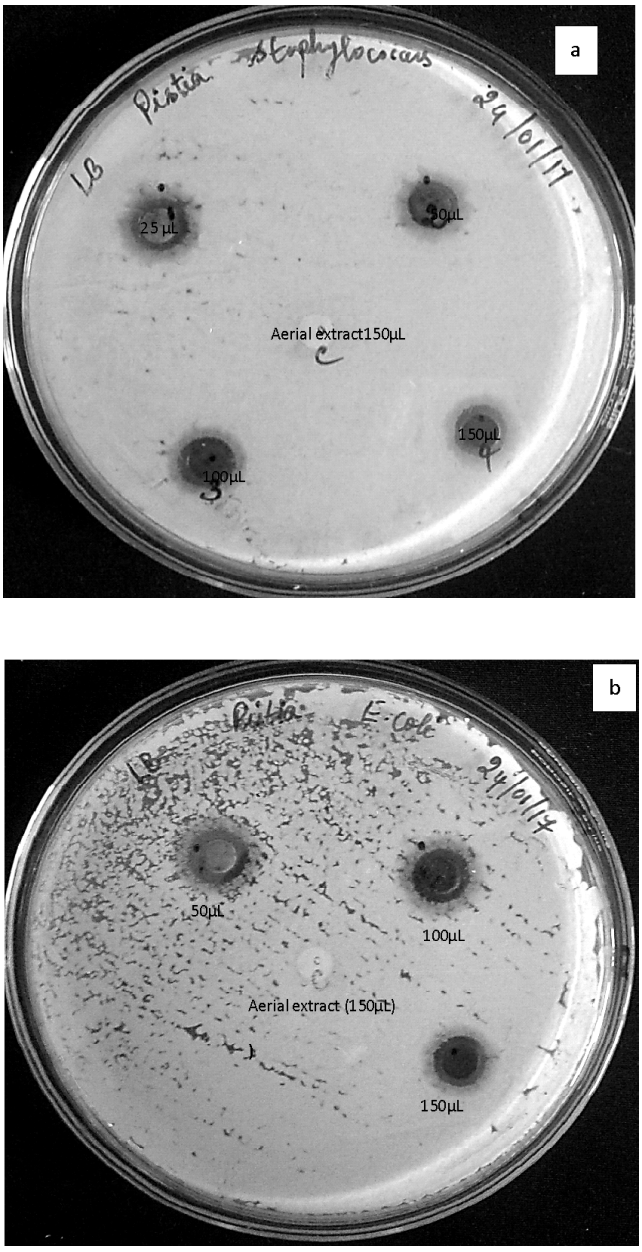

Fig. 10. Antibacterial activity of silver nanoparticles synthesized using extract of aerial part of *P. stratiotes* against (a) Gram (+) and (b) Gram (–) bacteria.

the reactant to overcome the kinetic barrier that exists due to the large potential difference between the donor and the acceptor.

Conclusion

Rapid synthesis of AgNPs using all the parts of the otherwise worthless weed Pistia (*Pistia stratiotes*) has been accomplished at normal temperature and pressure. Extracts from aerial and submerged parts of the plant were able to reduce Ag^{1+} to Ag^0 as well as stabilize the aggregating Ag atoms at the stage of nanoparticle formation. By using different plant parts and by varying their proportion with reference to the metal concentration, AgNPs of diverse geometry could be synthesized encompassing isotropic spherical and anisotropic triangular, pentagonal, hexagonal, and truncated triangular shaped particles of different sizes. The purity and the crystallinity of the synthesized AgNPs were confirmed by EDX, XRD and SAED studies. The FT-IR and EDX spectral studies together suggest that biomolecules amino acid residues and proteins were mainly involved in the reduction stabilization process. The synthesized AgNPs was seen to possess catalytic, antibacterial and antioxidant activity.

Acknowledgement

SAA thanks the University Grants Commission (UGC), New Delhi, for Emeritus Professorship and associated grants. SUG thanks the UGC for the Maulana Azad National Fellowship.

References

1. S. F. Adil, M. E. Assal, M. Khan, A. Al-Warthan, M. Rafiq, H. Siddiquia and L. M. Liz-Marzan, *Dalton Trans.,* 2015, **44**, 9709.
2. R. K. Ibrahim, M. Hayyan, M. A. Al-Saadi, A. Hayyan and S. Ibrahim, *Environ. Sci. Pollut. Res.*, 2016, **23**, 13754.
3. S. S. Sanjay and A. C. Pandey, *Advanced Structured Materials*, 2017, **62**, 47.
4. K. M. Metz, S. E. Sanders, J. P. Pender, M. R. Dix, D. T. Hinds, S. J. Quinn, A. D. Ward, P. Duffy, R. J. Cullen and P. E. Colavita, *ACS Sustainable Chem. Eng.*, 2015, **3**, 1610.
5. D. Sharma, S. Kanchi and K. Bisetty, *Arabian Journal of Chemistry,* 2015.
6. P. Singh, Y. J. Kim, D. Zhang and D. C. Yang, *Trends in Biotechnology*, 2016, **34(7)**, 588.
7. R. K. Das, S. K. Brar and M. Verma, *Trends in Biotechnology*, 2016, **34(6)**, 440.
8. M. Chung, I. Park, K. Seung-Hyun, M. Thiruvengadam

and G. Rajakumar, *Nanoscale Research Letters*, 2016, **11**, 40.

9. M. Shah, D. Fawcett, S. Sharma, S. K. Tripathy and G. E. J. Poinern, *Materials,* 2015, **8**, 7278.
10. S. Ahmed, M. Ahmad, B. L. Swami and S. Ikram, *J. Adv. Res.,* 2016, **7(1)**, 17.
11. V. V. Makarov, A. J. Love, O. V. Sinitsyna, S. S. Makarova, I. V. Yaminsky, M. E. Taliansky and N. O. Kalinina, *Acta Naturae*, 2014, **6**, 35.
12. K. Mittal, Y. Chisti and U. C. Banerjee, *Biotechnology Advances,* 2013, **31(2)**, 346.
13. S. Iravani, *Green Chem.,* 2011, **13**, 2638.
14. M. P. Patil and G. D. Kim, *Applied Microbiology and Biotechnology*, 2017, **101(1)**.
15. Z. ur R. Mashwani, M. A. Khan, T. Khan and A. Nadhman, *Advances in Colloid and Interface Science,* 2016, **234**, 132.
16. S. U. Ganaie, T. Abbasi, J. Anuradha and S. A. Abbasi, *Journal of King Saud University – Science,* 2014, **26**, 222.
17. M. V. Sujitha and S. Kannan, *Spectrochimica Acta - Part A : Molecular and Biomolecular Spectroscopy*, 2013, **102**, 15.
18. S. A. Abbasi and P. C. Nipaney, *Environmental Conservation,* 1986, **13(3)**, 235.
19. T. Abbasi and S. A. Abbasi, *Critical Reviews in Environmental Science and Technology,* 2011, **41(23)**, 2097.
20. C. Sarkar and S. A. Abbasi, *Environmental Monitoring and Assessment*, 2006, **119**, 201.
21. S. A. Abbasi, P. C. Nipaney and G. D. Schaumberg, *Biological Wastes*, 1990, **34(4)**, 359.
22. D. Mishima, M. Kuniki, K. Sei, S. Soda, M. Ike and M. Fujita, *Bioresource Technology,* 2008, **99**, 2495.
23. S. C. Anon, *International Journal of Bioresrouces, Environmental & Agricultural Sciences*, 2015, **1**, 132.
24. M. A. Bhat, T. Abbasi and S. A. Abbasi, *International Journal of Environmental Science and Engineering Research,* 2015, **6(2)**, 1.
25. N. Tripathi, A. M. Chandrasekaran Raichur and A. Mukherjee, *J. Biomed. Nanotechnology*, 2009, **5(1)**, 93.
26. S. Gajalakshmi, E. V. Ramasamy and S. A. Abbasi, *Biorescource Technology,* 2002, **82**, 165.
27. T. Abbasi and S. A. Abbasi, *Renewable and Sustainable Energy Reviews*, 2010, **14**, 1653.
28. S. A. Abbasi, M. Nayeem-Shah and T. Abbasi, *Journal of Cleaner Production,* 2015, **93**, 103.
29. APHA (American Public Health Association), Standard methods of water and wasterwater. 22nd ed., American Public Health Association, American Water Works Association and Water Environment Federation publication, Washington DC, USA, 2012.
30. S. U. Ganaie, S. Ravindran, T. Abbasi and S. A. Abbasi, *Journal of Nano Research,* 2015, **31**, 1.
31. S. U. Ganaie, T. Abbasi and S. A. Abbasi, *Particulate Science and Technology,* 2015, **33(6)**, 638.
32. J. Anuradha, T. Abbasi and S. A. Abbasi, *Journal of Advanced Research*, 2015, **6**, 711.
33. S. U. Ganaie, T. Abbasi, J. Anuradha and S. A. Abbasi, *Journal of King Saud Universify-Science,* 2014, **26**, 222.
34. D. Philip, *Spectrochimica Acta - Part A : Molecular and Biomolecular Spectroscopy,* 2010, **75**, 1078.
35. S. Sreelatha and P. R. Padma, *Plant Foods for Human Nutrition,* 2009, **64**, 303.
36. M. S. Abdel-Aziz, M. S. Shaheen, A. A. El-Nekeety and M. A. Abdel-Wahhab, *J. Saudi Chem. Soc.*, 2014, **18**, 356.
37. K. P. Singh, K. Bhardwaj, P. Dubey and A. Prabhune, *RSC Adv.*, 2015, **5**, 24513.
38. N. Muniyappan and N. S. Nagarajan, *Process Biochemistry*, 2014, **49(6)**, 1054.